The Optimization of Ejector Geometry for Mixing NaOH Powders with Water in On-board Carbon Solidification System

Haibin Wang[*], Saishuai Dai[*], Peilin Zhou[*, **]

* Department of Naval Architecture, Ocean and Marine Engineering, University of Strathclyde, 100 Montrose Street, Glasgow, G4 0LZ, UK, haibin.wang.100@strath.ac.uk, saishuai.dai@strath.ac.uk, peilin.zhou@strath.ac.uk.

** Zhejiang University, 1 Zheda Road, Zhoushan, Zhejiang Province, 316021, China

Abstract

Owing to increasing requirement of greenhouse gas emissions reductions, researchers all over the world has been investigating and developing technology applying to all different sectors. According to the report from International Maritime Organization (IMO), the international shipping has contributed 2.2% of global carbon emissions in 2012. To mitigate this situation, organizations, researchers and engineers are striving to reduce the emissions by increasing the energy efficiency or applying emission reduction regulations and techniques. Authors has investigated a chemical absorption method to absorb and solidify the carbon content in the exhaust gases from ships. In the chemical absorption method, to absorb the carbon dioxide from exhaust gases, sodium hydroxide (NaOH) solution is applied as absorbent. However, the storage of NaOH solution may cause stability and corrosion problems on ships. To eliminate these problem, this paper introduce the ejector technology to mix NaOH powders with water to supply and replenish absorbent to the system which will reduce the storage of NaOH solution and instead only NaOH powders should be stored on board. This paper also investigates the impact of swapping fluid inlets to determine a preferred design. With the application of design of experiment and computing fluid dynamic, the optimization of the preferred design is also carried out in order to determine an optimal design of the ejector geometry.

Keyword: CCS, Ejector geometry optimization, CFD, DOE.

1. Introduction

Since global warming effect has actual impact to humans' life, mitigation of climate change has become a popular topic which attracts researcher from all over the world to investigate and develop possible and potential solutions on it. Climate change has become a severe issue due to the growing of CO2 emissions. Figure 1 presents a trend line of global CO2 emissions due to fossil fuels combustion from 2000 to 2013 based on the recorded data from Carbon Dioxide Information Analysis Centre (Boden et al., 2010). According to IMO's report, the CO2 emission from international shipping is about 796 million tonnes in 2012, decreased from 885 million tonnes reported in 2007. The emission accounts for

about 2.2% of the global emission for 2012 (IMO, 2009; IMO, 2015). It is a result due to both global economic downturn and the adoptions of Energy Efficiency Design Index (EEDI) and the Ship Energy Efficiency Management Plan (SEEMP) in 2011 (IMO 2011). Many case study and analysis have been carried out applying EEDI to evaluate the energy efficiency of vessesls (Ozaki, 2011; Attah and Bucknall, 2015; Devanney, 2010). However, Bockmann and Steen accessed the EEDI of a general cargo vessel which indicates the attained EEDI value is 22% lower than actual CO2 emissions per transport work (Bockmann and Steen, 2016). Therefore, to comply with IMO's regulation, both the efforts from the design phase and the operation phase play a significant role. There are also many different technologies can be applied on ships for the sake of increasing energy efficiency and reducing the carbon emissions. A series of energy saving technologies have been investigated, such as coating, dual fuel engine and after treatment system. Demirel and his research team applied CFD simulation to access the resistance prediction with antifouling painting on ship hull (Demirel et al., 2014). Marques and Belchior developed a simple and rapid approach to help select suitable slow speed dual fuel engine in order to reduce the fuel consumption (Marques & Belchior, 2016). Authors has investigated an after treatment system to absorb the carbon emission from the exhaust gas with the help of laboratory experiment and CFD simulation (Zhou and Wang, 2014; Wang et al., 2016). Through experiment and simulation study and two case ship studies, it is believed that the carbon absorption and solidification method could meet the IMO's regulation to have 20% carbon reduction in 2020. However, due to additional equipment and material involved, the payback of the application depends on the sale of final products. Another issue is that, there are two different chemicals required to be in solution form which may lead to severe ship stability problem. To mitigate their effect, inspired by Yuan's research, ejector is considered to mix the powder with water to generate solution which increase the energy efficiency of the after treatment system (Yuan, 2014; Chen, 2017; Thongtip, 2017). There are already some research work done on the investigation of ejector. Arun and his team used CFD to investigate a rectangular cross-section ejector and however the analysis are not focusing on geometry designs (Arun et al., 2017). These papers indicate that the ejector could use the primary fluid to drive secondary fluid and to supply the mixture of two phases to the next process. The application has been considered and evaluated in refrigeration cycle by many researcher. It is reasonable to consider to apply ejector for mixing of chemical powders and water. With the aid of Design of Experiment and Computing Fluid Dynamic, this paper will investigate the application of ejector in the carbon absorption system, testing its functionality of mixing and optimizing the ejector geometry to achieve an optimal ejector design.

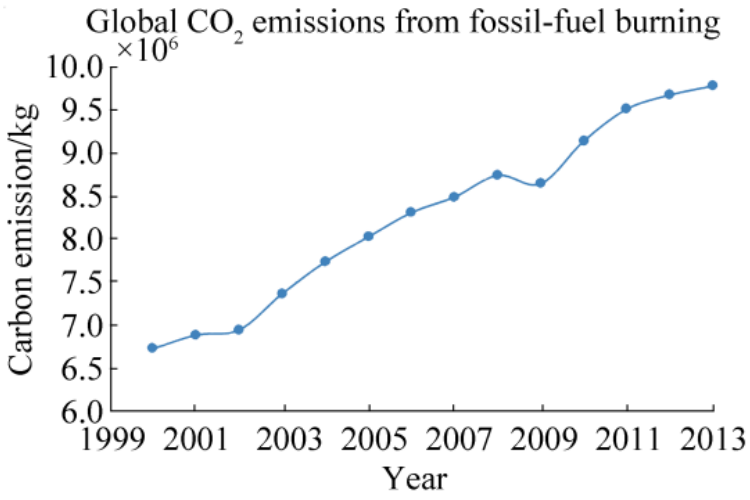

Fig. 1. Tendency of CO_2 emissions from 2000 to 2013

2. Methodology

2.1. Ejector principles

The basic principle of ejector is based on the Bernoulli's equation which is presented as the following:

$$\frac{v^2}{2} + gz + \frac{p}{\rho} = constant \quad (1)$$

where v is the fluid flow speed at a point on a streamline, g is the acceleration due to gravity, z is the elevation of the point above a reference plane, with the positive z-direction pointing upward – so in the direction opposite to the gravitational acceleration, p is the pressure at the chosen point, and ρ is the density of the fluid at all points in the fluid.

When the velocity of the fluid increased, the pressure will be decreased accordingly. When the ejector is working, the primary phase is pumped and driven by a pump/motor and gains a high velocity. Through the ejector, the primary fluid start to drive the air in the ejector to the outlet so the velocity of the inside air has been increased and the pressure decreased according to Bernoulli's equation. As a result, the pressure inside is lower than the secondary inlet and the secondary phase/fluid will be pumped into the ejector. Eventually, two phases will be mixed inside the chamber of ejector and released through the outlet. A general structure of an ejector is presented in Figure 2.

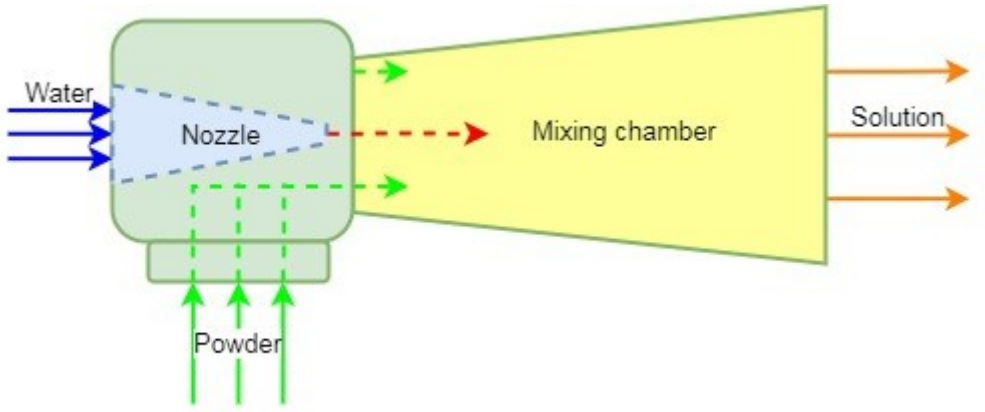

Fig. 2. Typical ejector structure.

2.2. Orthogonal design method

The orthogonal design method is an experimental process which can be applied to test and compare the effectiveness of multiple different factors on a target system or process. It is an efficient way to discover new phenomenon, materials or regular patterns during scientific researchand with these findings, research results can be developed to discover more meaningful results. Design of experiment (DOE) was established by Ronald Aylmer Fisher in the 1920s (Ronald, 1971). DOE was futher developed and improved by Genichi Taguchi's research team during 1940~1950 and the Taguchi methods were established. The orthogonal design method has been widely used in many different fields. Qiu et al. applied this method on their slewing bearing models to test the performance of connecting bolts while analysing siginificant factors (Qiu et al., 2011). The orthogonal design method is also applied to improve optimisation algorithms and find an optimal solution in Gong and his colleagues' research (Gong et al., 2008). Kim and his colleagues utilised the orthogonal design method to develop and test a dual phase steel. Three levels of three controllable factors were considered: intercritical annealing, aging and galvanizing temperatures during the heat treatment process (Kim et al., 2009).

The orthogonal design method will be applied to find out the impacts of the selected factors on the back pressure of powder inlet during the mixing process. The application of the orthogonal design method utilises a normalized table to the design experimens. It is an efficient, accurate and reliable way to discover optimal conclusions with a relatively small amount of trials. The selected factors are considered because they are important ones and are also controllable. A 4 factors by 5 level orthogonal design method table is designed as shown in Table 1.

Table 1. Orthogonal design method table for 4 factors with 5 levels

Design No.	L1	L2	L3	D1

1	1	1	1	1
2	1	2	2	2
3	1	3	3	3
4	1	4	4	4
5	1	5	5	5
6	2	1	2	3
7	2	2	3	4
8	2	3	4	5
9	2	4	5	1
10	2	5	1	2
11	3	1	3	5
12	3	2	4	1
13	3	3	5	2
14	3	4	1	3
15	3	5	2	4
16	4	1	4	2
17	4	2	5	3
18	4	3	1	4
19	4	4	2	5
20	4	5	3	1
21	5	1	5	4
22	5	2	1	5
23	5	3	2	1
24	5	4	3	2
25	5	5	4	3

2.3. CFD technology

For the CFD simulation, software Star-CCM+ is applied. The governing of equations are listed in the following paragraphs.

The balance of mass through a control volume is expressed by the continuity equation:

$$\frac{\partial \rho}{\partial t} + \nabla \cdot (\rho v) = 0 \qquad (2)$$

where ρ is the density and v is the continuum velocity.

The time rate of change of linear momentum is equal to the resultant force acting on the continuum:

$$\frac{\partial(\rho v)}{\partial t} + \nabla \cdot (\rho v \otimes v) = \nabla \cdot \sigma + f_b \quad (3)$$

where $\otimes$ denotes the Kronecker product, f_b is the resultant of the body forces (such as gravity and centrifugal forces) per unit volume acting on the continuum, and σ is the stress tensor. For a fluid, the stress tensor is often written as sum of normal stresses and shear stresses, σ=-pI+T, where p is the pressure and T is the viscous stress tensor, giving:

$$\frac{\partial(\rho v)}{\partial t} + \nabla \cdot (\rho v \otimes v) = -\nabla \cdot (pI) + \nabla \cdot T + f_b \quad (4)$$

3. Ejector Optimization

3.1. System description

The chemical process of carbon absorption system developed is presented in Figure 3. This figure presents both the locations and procedures of tanks in the system before storage tanks. These systems include a bypass system from funnel and a pipeline that transports the exhausted gas into absorption reaction tank. The fitting pipeline is in light blue colour. The green colour represents the absorption reaction tanks, and the pink and red ones are the precipitation tanks. The centrifuge separation system is denoted in dark blue, and the yellow ones indicate transportation. All the gravy compartments with grids indicate the ship hull and cargo hold.

Exhaust gases are bypassed and fed into the absorption system, and CO2 is trapped in the solution. The CO2-rich solution is transported to the precipitation tank, and CO2 is solidified into CaCO3. The mixture of sediment and solution is delivered into a centrifugation separation system through which the solution will be recycled for further absorption, and the sediment is transported and stored in storage tanks. The principles of the process are as follows:

CO_2 (g) + 2NaOH=Na_2CO_3+H_2O

Na_2CO_3 + CaO+H_2O=$CaCO_3$ (s) +2NaOH

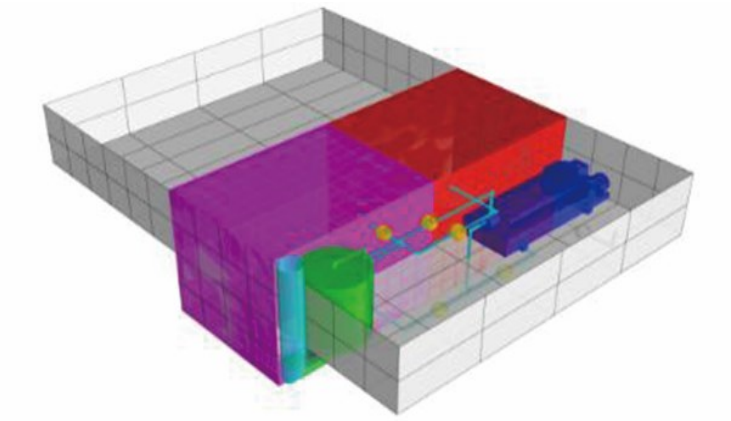

Fig. 3. CAD drawing of carbon absorption and solidification system in cargo hold

The application of ejector will take the advantage of water pump maximally in order to suck the chemical powder and mix it with pumped water. The modified system is presented as in Figure 4:

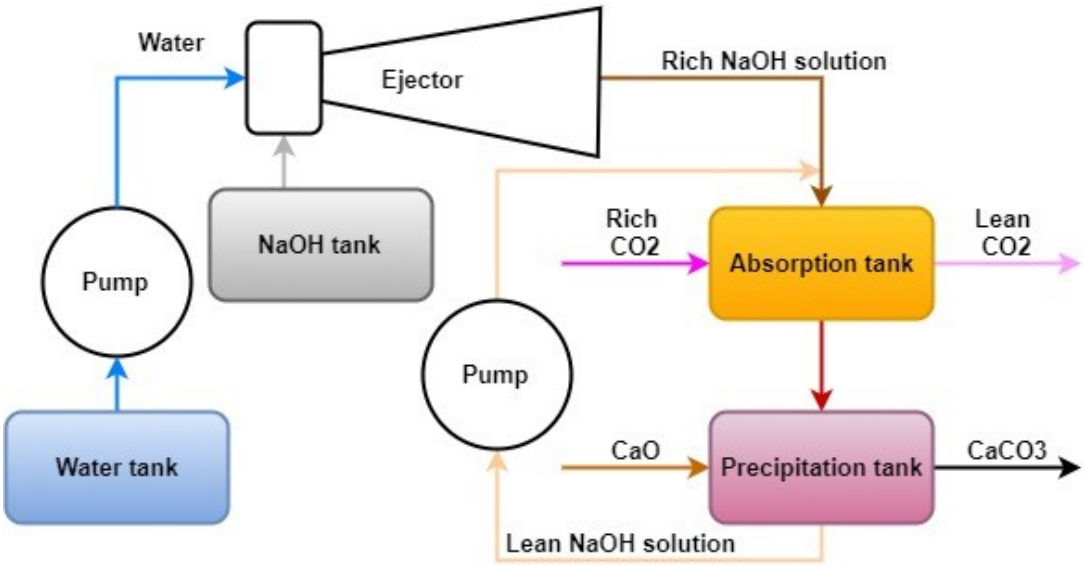

Fig. 4. Application of ejector in the chemical process for carbon absorption.

There are four parameters of ejector geometry analysed in this paper: length of the mixing chamber, length of the nozzle, length of particle path and the inside radius of the nozzle. The details of these parameters are presented in Figure 5 and the constraint are also shown in this figure.

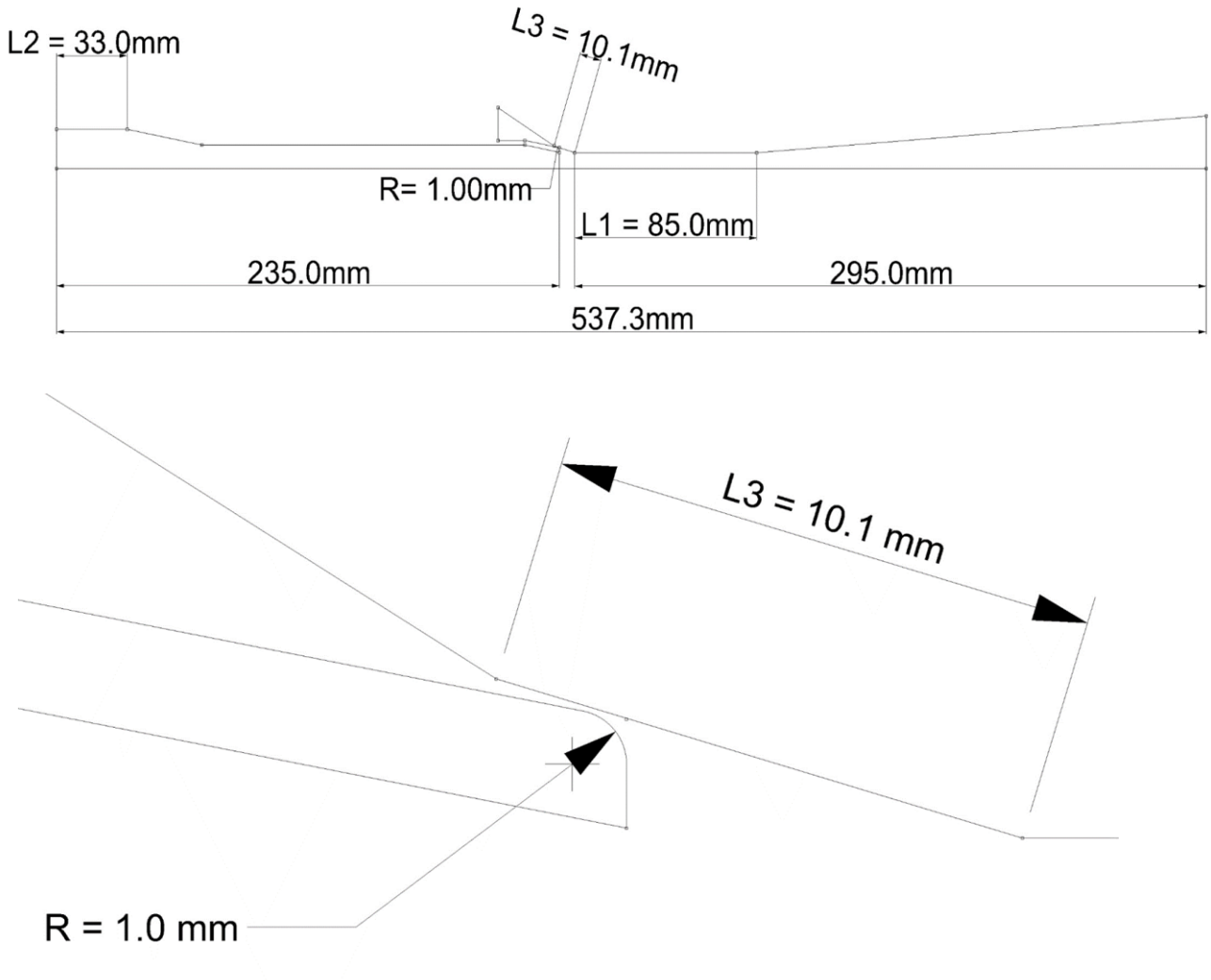

Fig. 5. Details of evaluated parameters

3.2. **CFD simulation**

Before carried out the simulation based on DOE, two different designs with swapped water inlet are assessed in order to determine the preferred design as a benchmark. The difference of two benchmark designs is the selection of inlets of primary phase (sea water) and secondary phase (powder). There are two different inlets in both design: inlet 1 and inlet 2. The initial design considered uses the inlet 1 for sea water and the inlet 2 is used for powder. Oppositely, the other design uses inlet 1 for powder driven by sea water from inlet 2. Figure 6 indicates these two different designs with also their pressure contours when reaching stable state and the results are presented in Table 2.

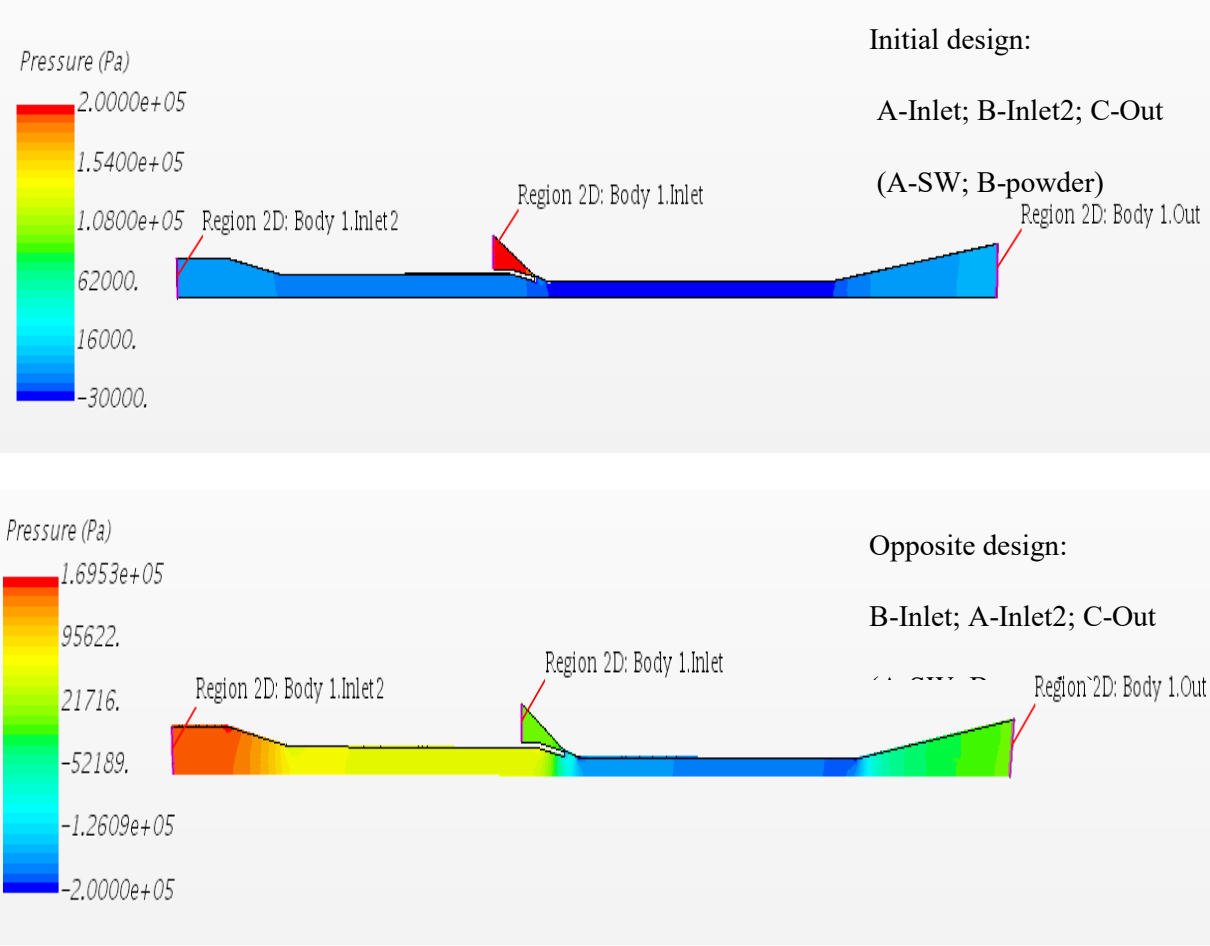

Fig. 6. Two different designs with pressure contours when reaching stable state.

Table 2. Simulation results of two different designs.

Parameters and results	Initial:	Opposite:
L1 (mm)	0.19	0.19
L2 (mm)	0.03	0.03
L3 (mm)	0.01	0.01
R (mm)	0	0
Initial pressure A (Pa)	200000	200000
End pressure A (Pa)	199723	153609
Initial pressure B (Pa)	0.00	0.00
End pressure B (Pa)	-3296	-176
Initial pressure C (Pa)	0.00	0.00
End pressure C (Pa)	0.00	-71
Surface average relative pressure at powder inlet (Pa)	-3296	-176
Velocity (m/s)	2.57	0.56

3.3. Design of experiment

DOE are applied to reduce the simulation and optimization times. Based on previous mentioned orthogonal table, a parameters table are designed and listed in Table 3. According to this table, 25 different designs of ejector geometry are presented and will be simulated and evaluated using CFD software.

Table 3. Geometry parameters in orthogonal design table

Design No.	L1	L2	L3	R
1	0.050	0.250	0.0050	0.00050
2	0.050	0.30	0.010	0.0010
3	0.050	0.350	0.0150	0.00150
4	0.050	0.40	0.020	0.0020
5	0.050	0.450	0.0250	0.00250
6	0.10	0.250	0.010	0.00150
7	0.10	0.30	0.0150	0.0020
8	0.10	0.350	0.020	0.00250
9	0.10	0.40	0.0250	0.00050
10	0.10	0.450	0.0050	0.0010
11	0.150	0.250	0.0150	0.00250
12	0.150	0.30	0.020	0.00050
13	0.150	0.350	0.0250	0.0010
14	0.150	0.40	0.0050	0.00150
15	0.150	0.450	0.010	0.0020
16	0.20	0.250	0.020	0.0010
17	0.20	0.30	0.0250	0.00150
18	0.20	0.350	0.0050	0.0020
19	0.20	0.40	0.010	0.00250
20	0.20	0.450	0.0150	0.00050
21	0.250	0.250	0.0250	0.0020
22	0.250	0.30	0.0050	0.00250
23	0.250	0.350	0.010	0.00050
24	0.250	0.40	0.0150	0.0010
25	0.250	0.450	0.020	0.00150

3.4. Ejector Optimization

As mentioned in previous section, the geometry parameters of ejector model considered are basically, the length of the mixing chamber, the length of particle path, the length of the nozzle and the inside radius of the nozzle. Based on the orthogonal design table, the CFD simulation results are derived and listed in Table 4. To evaluate the significance of parameters' impacts on the back pressure, a further analysis is carried out by comparing the extreme deviations for different parameters. The results are presented in Table 5 and it indicates that the rankings of parameters' significance is following: L2>L1>R>L3. It illustrates the relationships between parameters' variation and back pressure results which means with same variation in different parameters, the change of back pressure due to L1 variation is largest among all. Apart from the analysis on parameters variation, the optimal case can be found out from the CFD simulations. It is apparent that case 2 has the lowest pressure at 600s which is -1.00E+04Pa.

Table 4. CFD simulation results

Design set	L1 (m)	L2 (m)	L3 (m)	R (m)	Pressure (Pa)
1	0.250	0.0450	0.0250	0.00250	-1.94E+03
2	0.20	0.040	0.020	0.00250	-1.00E+04
3	0.150	0.0350	0.0150	0.00250	-3.68E+03
4	0.10	0.030	0.010	0.00250	-3.26E+03
5	0.050	0.0250	0.0050	0.00250	-3.44E+03
6	0.250	0.040	0.0150	0.0020	-7.49E+03
7	0.20	0.0350	0.010	0.0020	-4.02E+03
8	0.150	0.030	0.0050	0.0020	-2.40E+03
9	0.10	0.0250	0.0250	0.0020	-2.97E+03
10	0.050	0.0450	0.020	0.0020	-2.89E+03
11	0.250	0.0350	0.0050	0.00150	-3.75E+03
12	0.20	0.030	0.0250	0.00150	-3.02E+03
13	0.150	0.0250	0.020	0.00150	-2.12E+03
14	0.10	0.0450	0.0150	0.00150	-4.11E+03
15	0.050	0.040	0.010	0.00150	-9.89E+03
16	0.250	0.030	0.020	0.0010	-2.82E+03
17	0.20	0.0250	0.0150	0.0010	-1.95E+03
18	0.150	0.0450	0.010	0.0010	-4.09E+03

19	0.10	0.040	0.0050	0.0010	-9.42E+03
20	0.050	0.0350	0.0250	0.0010	-6.26E+03
21	0.250	0.0250	0.010	0.00050	-1.44E+03
22	0.20	0.0450	0.0050	0.00050	-3.00E+03
23	0.150	0.040	0.0250	0.00050	-6.04E+03
24	0.10	0.0350	0.020	0.00050	-3.37E+03
25	0.050	0.030	0.0150	0.00050	-3.69E+03

Table 5. Extreme deviations for different parameters

Significant	L1	L2	L3	R
Extreme deviation	1.74E+03	6.18E+03	4.97E+02	1.40E+03

After the simulation with the help of CFD, the analysis of impact of different parameters on back pressure is carried out. Firstly, the impact of the length of the mixing chamber is assessed. According to CFD results, Figure 7 is obtained which illustrates how the back pressure changed with the chamber length variation. It indicates that the mixing chamber has a negative effect on decreasing the back pressure and in another word the diffusion effect after mixing has more significant impact. However, to reach a suitable mixture in which NaOH powder is evenly distributed, the mixing chamber is necessary and trade-off between mixing and diffusion needs to be analysed in order to decrease pressure and keep a suitable mixture. Figure 8 shows the relationships between back pressure for powder inlet and nozzle length. This factor impacts the most among all the effects to the back pressure. The fact is that the longer the nozzle is, the closer the nozzle is to the mixing chamber. However, if the nozzle too close to the mixing chamber, the diameter for particle passing through will be decreased. Therefore the driven fluid entering the mixing chamber will be limited so that the driven effect will be mitigated. Figure 9 presents how the fluid path length impacts the pressure for powder suction. This parameter can slightly impact the back pressure by changing the contraction length. As a fact, when the contraction length is 0.01m, the back pressure reaches minimum. The impact of the inside radius of nozzle on powder suction pressure is illustrated in Figure 10. The optimal radius of nozzle is 0.001m and it indicates when selection of nozzle, its inner radius should be well considered because it will impact the final back pressure on the powder suction. From these figures, the optimal values for each parameters with the minimum back pressure are determined. After combining these parameters, the optimal case from analysis is determined and presented together with the optimal case from CFD simulation in Table 6. After CFD simulation based on the optimal design from analysis, the result of back pressure for the powder suction is derived. Comparing with these two results, it is obvious that these two cases have a similar back pressure. Especially, the nozzle position plays a dominate role in decreasing the back

pressure. Therefore, this design is recommended for the practical design of the ejector which will be applied for carbon absorption system.

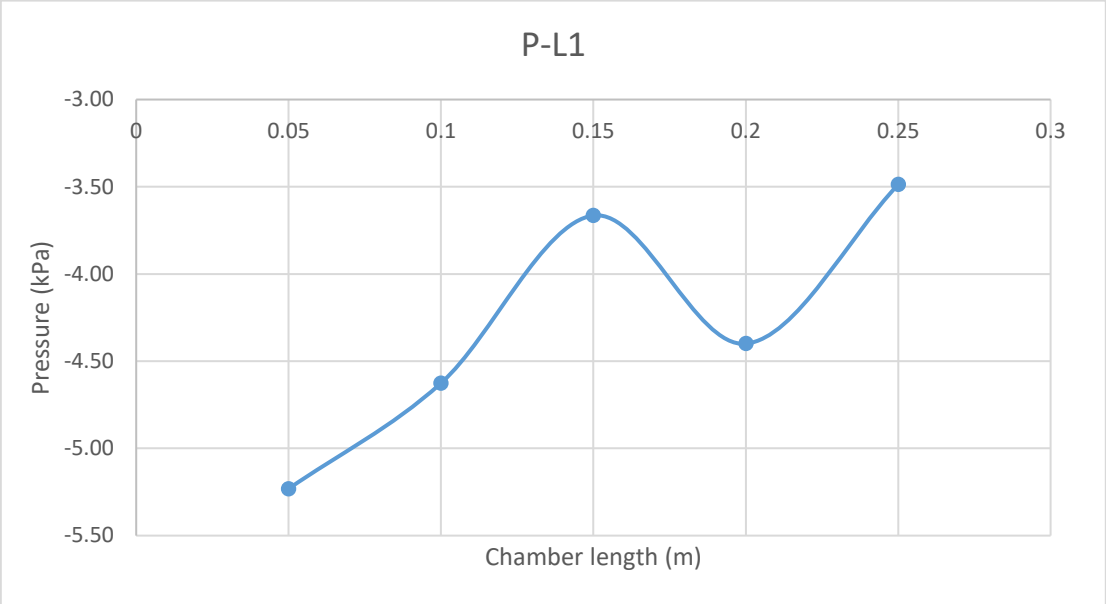

Fig. 7. Back pressure changed with the chamber length variation.

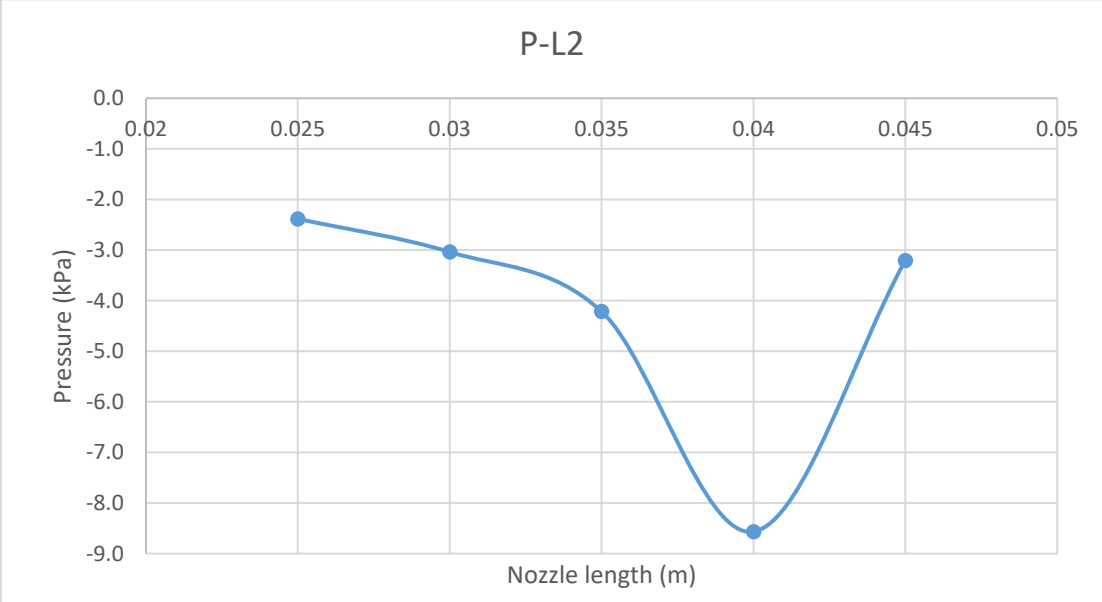

Fig. 8. Back pressure changed with length variation of the nozzle.

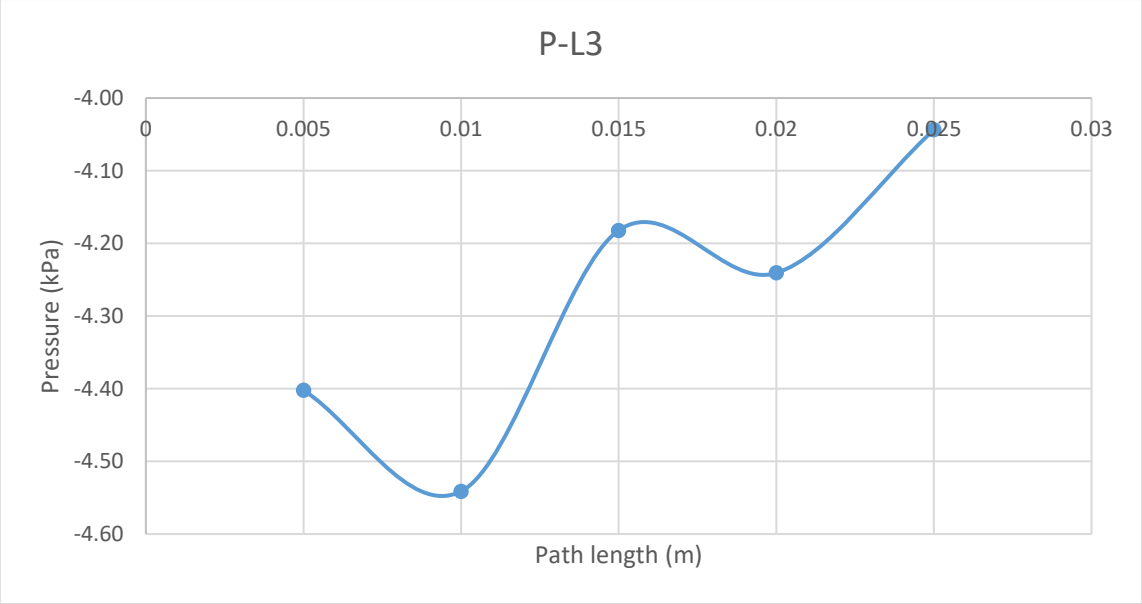

Fig. 9. Back pressure changed with the length variation of the fluid path.

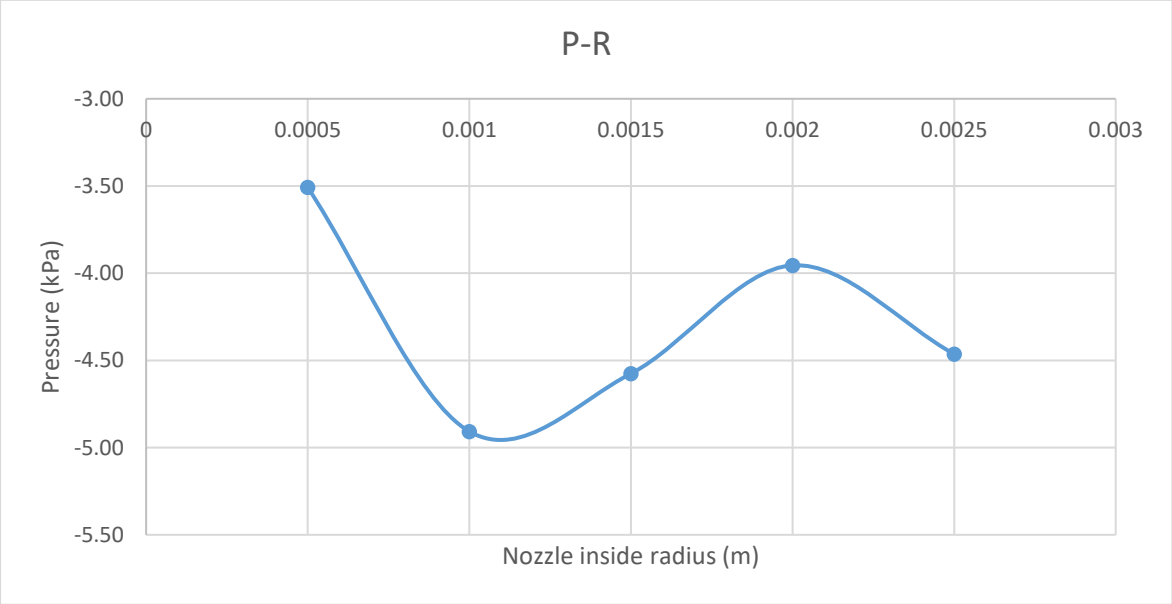

Fig. 10. Back pressure changed with the inside radius variation of the nozzle

Table 6. Geometry parameters of optimal case

Optimal case	L1	L2	L3	R	Pressure results
Case 2	0.20	0.040	0.020	0.00250	-10002.33
From analysis	0.050	0.040	0.010	0.0010	-10002.14

4. Conclusions

This paper investigate the application of ejector in chemical process for carbon absorption in order to reduce the energy requirement from the pumping/transferring fluids and mixing with water. The principle of combining the ejector into the system has been presented. To achieve the optimal benefit from ejector application, CFD simulation was applied to evaluate different designs and the impacts of geometric parameters on the back pressure for powder suction. With the help of DOE technique, the total simulation runs have been dramatically reduced. After further analysis on the simulation results, the significant ranking of the geometric parameter impacts is derived and the position of the nozzle in the ejector has the most significant influence. Therefore an optimal design has been obtained based on these analysis which provides a minimum back pressure to drive the powder for mixing and supplying to the absorption system. Further studies will be focused on evaluation of the effect of energy saving due to the installation of ejector. Also the mixing effect should be considered in further research works in order to assess the overall performance of the ejector.

References

Arun, K., Tiwari, S. and Mani, A., (2017). Three-dimensional numerical investigations on rectangular cross-section ejector, International Journal of Thermal Sciences, 2017 vol: 122 (Supplement C) pp: 257-265, DOI: https://doi.org/10.1016/j.ijthermalsci.2017.08.024, ISSN: 1290-0729

Attah, E. and Bucknall, R., (2015).An analysis of the energy efficiency of LNG ships powering options using the EEDI, In Ocean Engineering, Volume 110, Part B, 2015, Pages 62-74, ISSN 0029-8018, https://doi.org/10.1016/j.oceaneng.2015.09.040.

Bøckmann, E. and Steen, S., (2016). Calculation of EEDIweather for a general cargo vessel, Ocean Engineering 2016 vol: 122 (Supplement C) pp: 68-73, DOI: https://doi.org/10.1016/j.oceaneng.2016.06.007, ISSN: 0029-8018

Boden, T.A., Marland, G. and Andres, R.J., (2010). Global, regional, and national fossil-fuel CO2 emissions. Carbon Dioxide Information Analysis Centre, Oak Ridge National Laboratory, U.S. Department of Energy, Oak Ridge. DOI: 10.3334/CDIAC/00001_V2010

Chen, Z., Jin, X., Shimizu, A., Hihara, E. and Dang, C., (2017). Effects of the nozzle configuration on solar-powered variable geometry ejectors, Solar Energy, 2017 vol: 150 (Supplement C) pp: 275-286, DOI: https://doi.org/10.1016/j.solener.2017.04.017, ISSN:0038-092X

Demirel, Y., Khorasanchi, M., Turan, O., Incecik, A. and Schultz, M., (2014). A CFD model for the frictional resistance prediction of antifouling coatings, Ocean Engineering, 2014 vol: 89 (Supplement C) pp: 21-31, DOI: https://doi.org/10.1016/j.oceaneng.2014.07.017, ISSN:0029-8018

Devanney, J.and Beach, S., (2010). EEDI, A Case Study in Indirect Regulation of CO2 Pollution

Gong, W.Y., Cai, Z.H. and Jiang, L.X., (2008). Enhancing the Performance of Differential Evolution Using Orthogonal Design Method, Applied Mathematics and Computation 206 (2008) 56–69, doi:10.1016/j.amc.2008.08.053.

IMO, (2009). Second IMO Greenhouse Gas Study 2009

IMO, (2011). Amendments to the annex of the protocol of 1997 to amend the international convention for the prevention of pollution from ships, 1973, as modified by the protocol of 1978 relating thereto (Inclusion of regulations on energy efficiency for ships in MARPOL Annex VI)

IMO, (2015). Third IMO Greenhouse Gas Study 2014

Kim, S.J., Cho, Y.G., Oh, C.S., Kim, D.E., Moon M.B., and Han, H.N., (2009). Development of a Dual Phase Steel Using Orthogonal Design Method, Materials and Design 30 (2009) 1251–1257, doi:10.1016/j.matdes.2008.06.017.

Marques, C. and Belchior, C., (2017). Optimised selection of marine dual-fuel low-speed diesel engines: introducing relative specific fuel consumptions, Marine Systems and Ocean Technology, 2017 vol: 12 (1) pp: 1-12, DOI: 10.1007/s40868-016-0019-6, ISSN:2199-4749

Ozaki, Y., Larkin, J., Baker, C., Tikka, K. and Michel, K, (20110. An Evaluation of the Energy Efficiency Design Index (EEDI) Baseline for Tankers, Containerships, and LNG Carriers

Qiu, M., Yan J.F., Zhao, B.H., Chen, L., and Bai, Y.X., (2011). A Finite-Element Analysis of the Connecting Bolts of Slewing Bearings Based on the Orthogonal Method, Journal of Mechanical Science and Technology 26 (3) (2012) 883~887, DOI 10.1007/s12206-011-1203-4.

Ronald, A.F., (1971). The Design of Experiments, Hafner Publishing Company, New York, 1971.

Thongtip, T. and Aphornratana, S., (2017). An experimental analysis of the impact of primary nozzle geometries on the ejector performance used in R141b ejector refrigerator, Applied Thermal Engineering, 2017 vol: 110 (Supplement C) pp: 89-101, DOI: https://doi.org/10.1016/j.applthermaleng.2016.08.100, ISSN: 1359-4311

Wang, H., Zhou, P. and Wang, Z., (2016). Experimental and numerical analysis on impacts of significant factors on carbon dioxide absorption efficiency in the carbon solidification process, Ocean Engineering, 2016, Volume 113, Pages 133-143, DOI: 10.1016/j.oceaneng.2015.12.036, ISSN: 00298018

Yuan, H., Mei, N. and Zhou, P., (2014). Performance analysis of an absorption power cycle for ocean thermal energy conversion, Energy Conversion and Management, 2014 vol: 87 (Supplement C) pp: 199-207, DOI: https://doi.org/10.1016/j.enconman.2014.07.015, ISSN:0196-8904

Zhou, P. and Wang, H., (2014). Carbon capture and storage—Solidification and storage of carbon dioxide captured on ships, Ocean Engineering, 2014 Volume 91 Pages 172-180, DOI: 10.1016/j.oceaneng.2014.09.006, ISSN: 00298018